RSC Advances

Solution phase synthesis of homogeneously alloyed ultrathin CdSxSe1-x Nanosheets

Journal:	*RSC Advances*
Manuscript ID:	RA-COM-09-2014-010559
Article Type:	Communication
Date Submitted by the Author:	16-Sep-2014
Complete List of Authors:	Maiti, Pradipta Sankar; Ben Gurion University of the Negev, Chemistry Meir, Noga; Weizmann Institute of Science, Physics Houben, Lothar; Forschungszentrum Juelich GmbH, Peter Grünberg Institute and Ernst Ruska-Centre for Microscopy and Spectroscopy with Electrons Bar Sadan, Maya; Ben Gurion University of the Negev, Department of chemistry

RSC Advances

RSCPublishing

COMMUNICATION

Solution phase synthesis of homogeneously alloyed ultrathin CdS_xSe_{1-x} Nanosheets

Cite this: DOI: 10.1039/xoxxoooooox

Pradipta Sankar Maiti[a], Noga Meir[b], Lothar Houben[c] and Maya Bar-Sadan[a]*

Received ooth January 2012,
Accepted ooth January 2012

DOI: 10.1039/xoxxoooooox

www.rsc.org/

Provided that precise control could be achieved over their optoelectronic properties, semiconductor two-dimensional (2D) nanosheets with a thickness of a few monolayers would constitute appealing building blocks. It is well established that alloying promotes efficient bandgap engineering, but divergent precursor reactivities have so far prevented the production of homogeneously alloyed 2D structures. We report a simple synthesis of alloyed CdS_xSe_{1-x} that preserves the 2D nature. High resolution microscopy reveals their edge structure and atomic rearrangement within the layer. Their optical properties show a comparable or higher quantum yield relative to pure nanosheets, making them promising materials for various applications.

Newly discovered two-dimensional (2D) semiconductor colloidal nanosheets show strong quantum confinement in the one-dimensional regime.[1] Tuning of their optical and electronic properties requires precise control over size, composition and morphology. Recent studies have already demonstrated that they possess appealing properties, e.g. low-threshold amplified emission.[2] Prospective applications include monochromatic LEDs, large area photovoltaics, and optical sensors.

Common strategies for tuning the electronic and optical properties of nanosheets include control of their thickness at the atomic level 3 or deposition of another material with a higher bandgap.[4] Additional deposition of a second semiconductor such as CdS and CdZnS[5] is a cumbersome process where the challenge is to maintain the 2D morphology while precisely controlling the thickness at the atomic level. Alternatively, tunable optical properties can be achieved by alloying in a one-pot synthesis, for example CdS_xSe_{1-x} with different Se:S ratios.[6] However, due to the diverse reactivities of the commonly used S and Se precursors, obtaining homogeneous 2D alloys requires a delicate synthesis; to the best of our knowledge, such a synthesis has not been performed successfully so far.

In this work we present the low-temperature solution phase synthesis of homogeneous ultrathin alloyed CdS_xSe_{1-x} nanosheets using a mixture of S-Se precursors. We show that the alloyed samples preserve the 2D geometry of the pure samples but offer better optical properties such as quantum yield (QY). We use high resolution transmission electron microscopy (TEM) to uncover structural features that can explain the optical properties.

We initially tried to synthesize homogeneous alloys by simply using mixtures of S and Se in the amine solvents, but that approach resulted in a few large 2D nanosheets and several undefined smaller nanostructures (Figure S1). To our understanding, the key to obtaining homogeneous nucleation and growth of the alloy compounds is efficient mixing of the precursors prior to cluster nucleation, which is facilitated through the creation of suitable complexes. We succeeded in producing homogenous alloyed nanosheets by balancing the precursors' reactivity similar to the production of alkylammonium selenide complexes by reduction of Se in the presence of $NaBH_4$, octylamine and oleylamine[7] (see the supporting information for detailed description of all syntheses protocols).

Pure CdS and CdSe 2D nanosheets were synthesized according to modified procedures based on refs 8a,b. In general, the Cd precursor was a $CdCl_2(amine)_2$ complex and the anion source is a Se(amine) or S(amine) complex. Transmission electron microscope (TEM) pictures of the purified products show ultrathin nanosheets with lateral dimensions ranging from 20 nm to a few hundreds of nanometers (Figures 1a and 1e). The corresponding scanning transmission electron microscope (STEM) images (Figures 1f and 1j) are characterized by uniform contrast, indicating uniform thickness across the nanosheets. Additional TEM images of both pure and alloyed samples can be found in the Supporting Information (see Figure S2).

In order to produce homogenous alloys, we prepared the reactive S-Se precursor by reducing the calculated amount of S and Se with $NaBH_4$ as mentioned above, with several S/Se ratios. Figures 1b-d present samples with ratios of $CdS_{0.6}Se_{0.4}$, $CdS_{0.4}Se_{0.6}$ and $CdS_{0.3}Se_{0.7}$. The samples contained 2D nanosheets with various

aspect ratios and with a typical width of 20-40 nm and length of several hundreds of nanometers. In the samples with lower Se content we observed also small quantities of branched structures; however as the Se content was increased the production of such branched structures was inhibited.

Atomic resolution aberration-corrected TEM was carried out in low voltage (80kV) in order to minimize radiation damage. Figure 2a shows a $CdS_{0.3}Se_{0.7}$ nanosheet in high resolution with a large field of view. The nanosheets of the alloyed samples and pure compounds were all in the hexagonal wurtzite crystallographic phase, as described in Ref. 9.

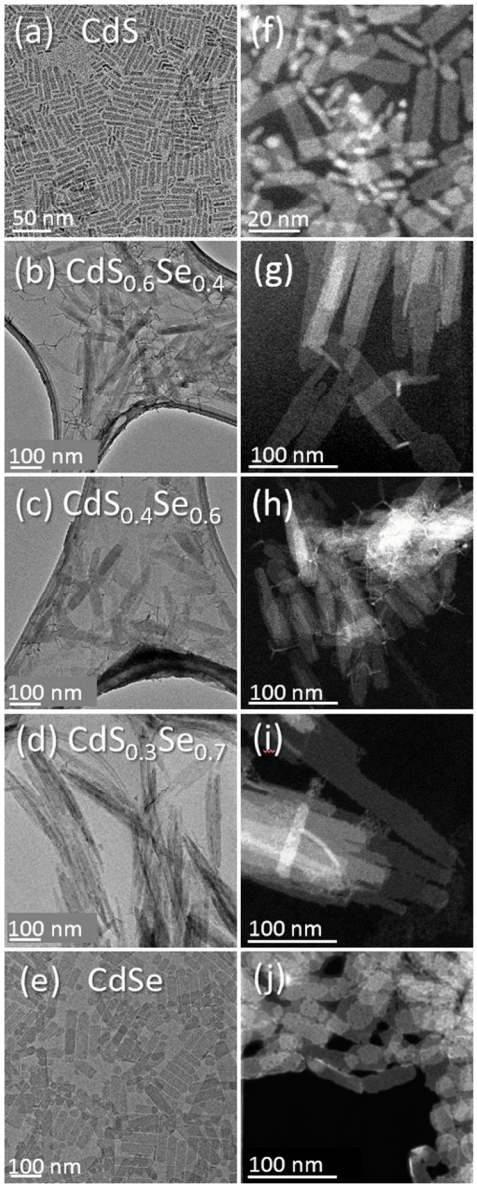

Figure 1. Representative bright-field TEM images of 2D CdS_xSe_{1-x} (a-e) and corresponding STEM high-angle annular dark field images (f-j). The nanosheets are composed of CdS, $CdS_{0.6}Se_{0.4}$, $CdS_{0.4}Se_{0.6}$, $CdS_{0.3}Se_{0.7}$ and CdSe.

In order to make the crystallographic structure more prominent, the image in Figure 2a was Fourier-filtered using the (1-100) reflection; the result is presented in Figure 2b, highlighting only the areas of coherent hexagonal domains. The white arrows on the image point to stacking faults, a linear defect of the atomic planes in the [00-1] direction. The domains between the stacking faults can be as wide as 30 nm, or they can be close together as seen to the right edge of the image. Although the overall appearance is quite uniform, the edges show irregularities and in some areas there is a hole in the structure, marked by the dotted white circle. Such a structure supports a reaction mechanism of oriented attachment of small patches, as was suggested in the literature.[10] The atomic resolution STEM image, presented in Figure 2c, allows direct interpretation of the atomic structure of a $CdS_{0.4}Se_{0.6}$ nanosheet. Cd columns are brighter than S/Se columns (see the atomic model overlaid on the image). A stacking fault can be also seen and it is marked by the white arrow and the dotted line.

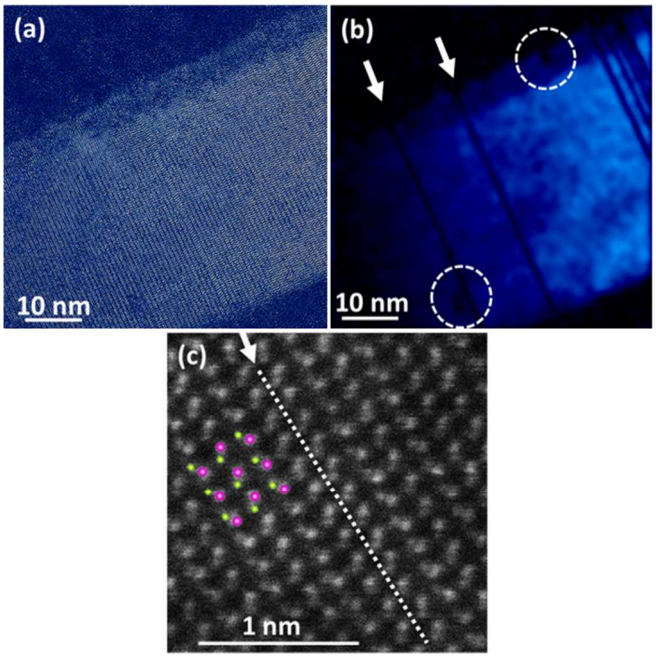

Figure 2. (a) Aberration corrected HRTEM image of an individual $CdS_{0.3}Se_{0.7}$ nanosheet (contrast enhanced and false-coloured to guide the eye). (b) Fourier filtered image, constructed with the (1-100) reflection. The white arrows mark a stacking fault in the nanosheet. The white dotted circles indicate areas of crystallographic disorder or a hole in the structure. (c) Atomic-resolution STEM high-angle annular dark field image of a $CdS_{0.4}Se_{0.6}$ nanosheet. The atomic model structure is overlaid on the image, Cd in magenta and S/Se in green. The white arrow and the dotted line indicate a stacking fault in the structure.

The evolution of the crystal structure with varying composition was examined by powder X-ray diffraction (XRD). Each XRD pattern (see Figure 3a) consisted of a set of 2Θ peaks corresponding to the hexagonal wurtzite structure. The diffraction peaks shifted gradually toward smaller angles with increased substitution of S atoms by the bigger and heavier Se atoms. The calculated lattice parameters for pure CdS nanosheets from the XRD spectrum were a = 0.410 nm and c = 0.667 nm, indicating a contraction of 0.8% from bulk hexagonal CdS, which is typical to Cd based nanoparticles.[11] The smeared spectrum of pure CdSe nanosheets (similar to reference 8b) did not allow direct calculation of the lattice parameters but only

of the ratio c/a, which was found to be 1.62. Alloyed samples exhibited intermediate values between CdS and CdSe, e.g. $CdS_{0.3}Se_{0.7}$ nanosheets showing lattice parameters of a = 0.426 nm and c = 0.689 nm. According to Vegard's law, an alloy composed of homogenous solid solution exhibits linear relation, at constant temperature, between the crystal lattice parameter of the alloy and the concentrations of its constituent elements. The calculated lattice parameters of the alloyed samples were in accordance with Vegard's law, and the c/a ratio was found to be 1.62 for both pure and alloyed samples, indicating the formation of homogenous alloys.

In order to verify the composition of the nanosheets, Energy Dispersive X-Ray Spectroscopy (EDS) measurements were performed for elemental analysis (see table S1). The EDS data confirmed that the actual composition of the CdS_xSe_{1-x} nanosheets was slightly more Se-rich in comparison to the injected Se–S stock solution. This finding suggests that under the given synthetic conditions, Se still preserves more reactivity towards cadmium compared to S. However, the distributions of elements Cd, S and Se in the nanosheets were very homogeneous, which can be confirmed by electron energy loss spectroscopy (EELS) elemental mapping (Figure S3).

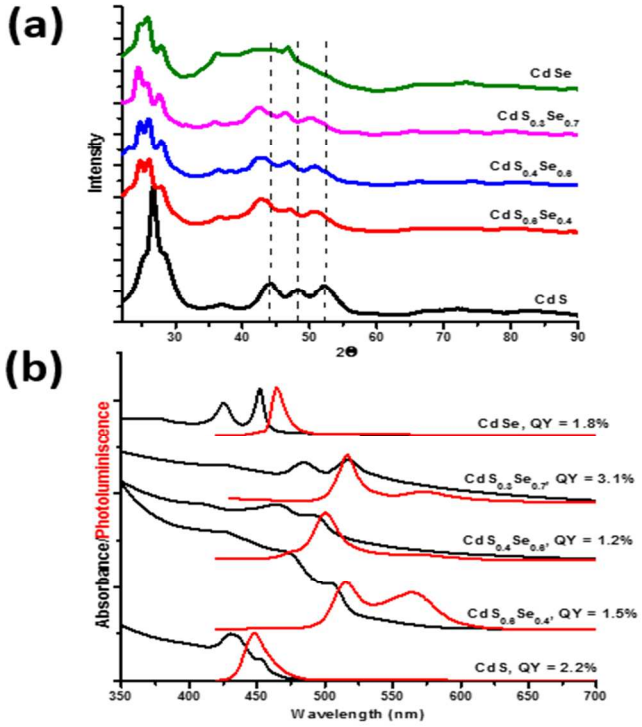

Figure 3. XRD patterns of the 2D nanosheets. The shift of XRD peaks indicates gradual contraction of the lattice with increased Se content. (a). UV-visible spectra and corresponding photoluminescence spectra of the CdS_xSe_{1-x} nanosheets recorded in chloroform solution in room temperature (b).

The UV/Vis absorption spectra of the CdS_xSe_{1-x} nanosheets and their corresponding photoluminescence (PL) spectra are shown in Figure 3b. Both are similar to previously reported spectra of CdSe nanoribbons, nanoplatelets, and nanosheets, all of which have thicknesses comparable to the CdS_xSe_{1-x} described here, and hence they support the 2D structure of the nanosheets. As described in previous works [12], we assigned the three absorption peaks from lower to higher energy to 1_{hh}-1_e, 1_{lh}-1_e, and 2_{hh}-2_e quantum well transitions, respectively (*hh* ≡ heavy hole, *lh* ≡ light hole, and *e* ≡ electron) [3]. In the case of the pure CdSe nanosheets, the 1_{hh}-1_e, 1_{lh}-1_e, and 2_{hh}-2_e transitions occur at 452 nm (2.74 eV), 425 nm (2.92 eV) and 374 nm (3.32 eV), respectively. Such an interpretation could not be applied to the pure CdS samples, as here the 1_{hh}-1_e, 1_{lh}-1_e transitions are superimposed around the peak at 431 nm. For an exemplary case, $CdS_{0.3}Se_{0.7}$, the 1_{hh}-1_e, 1_{lh}-1_e, and 2_{hh}-2_e transitions occur at 517 nm, 484 nm and 422 nm, respectively. Thus the optical absorption spectra suggest that these CdS_xSe_{1-x} nanosheets are also 2D structures that exhibit quantum-confinement effects associated with the reduced dimensions of the thickness. The data reported here for pure CdSe samples indicate 5 monolayer thick nanosheets.[8b] However, the spectra of the alloyed samples are red-shifted to higher wavelengths (lower energies) relative to both pure compounds.

The normalized PL spectra of all the samples showed an emission band related to near-bandedge recombination. The PL spectrum of the pure CdS and CdSe nanosheets showed an extremely narrow peak, with full width at half maximum (FWHM) as small as 20 nm at 448 nm for CdS and 11 nm at 464 nm for CdSe. Such narrow FWHM values indicate extremely uniform thickness of the nanosheets. The alloyed samples showed broader features, and the spectral peaks for these ultrathin nanosheets shifted towards low energy with varying Se amount – from 448 nm to 517 nm, which also represents red-shifting relative to both pure compounds. In the cases of $CdS_{0.3}Se_{0.7}$ and $CdS_{0.6}Se_{0.4}$, the PL spectra contained an additional low-energy emission peak associated with a defect or structural disorder, as could be predicted from the HRTEM measurements presented in Figure 2. It is worth mentioning that the bandedge emission of these ternary CdS_xSe_{1-x} nanosheets is very strong at room temperature, pointing to potential applications in adjustable optoelectronic devices in the visible region.

To evaluate the optical quality of the CdS_xSe_{1-x} nanosheets, we measured their absolute QY in dilute chloroform solution at room temperature. We found that the QY ranged from 1.2% to 3.1%. For $CdS_{0.3}Se_{0.7}$ nanosheets the measured QY was high (~3.1%) relative to pure CdS (~2.2%) and CdSe (~1.8%) nanosheet samples.

The optical properties of homogeneous alloyed samples may be expected to lie somewhere between those of the pure binary compounds, as in the particular case of the Vegard law for the lattice parameters. In the present study, the optical properties of the alloyed samples were positioned beyond both pure compounds and were red-shifted in both the absorbance and the PL spectra. However, the underlying assumption is that the structures remained the same and only the chemical composition underwent a change. A plausible explanation for the red shift observed here may be arrived at by setting the absorbance spectra against the data in the literature regarding thicker samples comprising 6 monolayers. It is probable that the alloyed samples are indeed one monolayer thicker than the pure compounds, in which case it would be misleading to compare the optical properties of the pure and alloyed samples directly. Corroborating evidence is provided by AFM height measurement (Figure S4 and Table S3): 4.0 nm for the nanosheets and their capping organic layers, or 1.8 nm for the $CdS_{0.3}Se_{0.7}$ nanosheets themselves, which agrees with a 6 monolayer thick structure. For the $CdS_{0.6}Se_{0.4}$ and $CdS_{0.4}Se_{0.6}$, the measured thickness is 1.6 nm, corresponding with a 5-6 monolayer thick samples.

It has already been established that in the case of pure CdS and CdSe nanosheets, bandedge emission exhibits a red shift and a QY

decrease as the number of atomic layers increases[3]. In the present work, it was encouraging to see that the alloyed nanosheets, although thicker and somewhat disordered, provided a comparable or higher QY relative to the pure compounds, as seen for $CdS_{0.3}Se_{0.7}$. A better understanding of the structure-properties relationship and the reaction mechanism governing the growth of these nanosheets will require precise high resolution TEM measurements; these lie beyond the scope of the present communication.

In conclusion, we have devised a simple and robust process for the solution phase synthesis of two-dimensional CdS_xSe_{1-x} nanosheets with thickness control at the atomic level. By varying the S and Se precursor ratio during the synthesis, we were able to tune their optical bandgap and emission properties. The alloyed CdS_xSe_{1-x} nanosheets were probably one monolayer thicker than the pure compounds, but their quantum yield was comparable to or higher than that of their pure counterparts. Atomic resolution TEM revealed large domains of wurtzite phase measuring up to a few dozens of nm. Surface and disorder states apparent in the optical absorption spectra could be associated with the edge structure and occasional perforated holes. Precise control of both the optical and excited state properties of the ultrathin CdS_xSe_{1-x} nanosheets will pave the way to applications in the fields of optoelectronics and photovoltaics.

Acknowledgements. This research project was supported by The Israeli Centers of Research Excellence (I-CORE) program, (Center No. 152/11), ISF grant 475/12, and the European Union Seventh Framework Programme, under Grant Agreement 312483 - ESTEEM2 (Integrated Infrastructure Initiative–I3). M.B.S. appreciates support from Dr. Vladimir Ezersky, Dr. Dmitri Mogilyanski and Roxana Golan of the Ilse Katz Institute for Nanoscale Science Technology.

Notes and references

[a] Department of Chemistry and the Ilse Katz Institute Ben Gurion University P.O.B. 653 Beer-Sheva, 8410501 Israel, Email: barsadan@bgu.ac.il
[b] Department of Physics, Weizmann Institute of Science, 234 Herzl St., Rehovot 7610001, Israel.
[c] Peter Grünberg Institute and Ernst Ruska-Centre for Microscopy and Spectroscopy with Electrons,
Forschungszentrum Jülich GmbH
52425 Jülich, Germany

Electronic Supplementary Information (ESI) available: synthesis protocol and additional characterization data. See DOI: 10.1039/c000000x/

1. a) S. Ithurria, B. Dubertret, *J. Am. Chem. Soc.* 2008, **130**, 16504; b) J. Joo, J. S. Son, S. G. Kwon, J. H. Yu, T. Hyeon, *J. Am. Chem. Soc.* 2006, **128**, 5632; c) Z. Li, X. Peng, *J. Am. Chem. Soc.* 2011, **133**, 6578; d) M. D. Tessier, P. Spinicelli, D. Dupont, G. Patriarche, S. Ithurria, B. Dubertret, *Nano Lett.* 2014, **14**, 207.
2. a) C. She, I. Fedin, D. S. Dolzhnikov, A. Demortière, R. D. Schaller, M. Pelton, D. V. Talapin, *Nano Lett.* 2014, **14**, 2772. b) B. Guzelturk, Y. Kelestemur, M. Olutas, S. Delikanli, H. V. Demir, *ACS Nano* 2014, **8**, 6599.
3. S. Ithurria, M. D. Tessier, B. Mahler, R. P. S. M. Lobo, B. Dubertret, Al. L. Efros, *Nat. Mater.* 2011, **10**, 936.
4. S. Ithurria, D. V. Talapin, . *J. Am. Chem. Soc.* 2012, **134**, 18585.
5. B. Mahler, B. Nadal, C. Bouet, G. Patriarche, B. Dubertret, *J. Am. Chem. Soc.* 2012, **134**, 18591.
6. a) L. A. Swafford, L. A. Weigand, M. J. Bowers, J. R. McBride, J. L. Rapaport, T. L. Watt, S. J. Rosenthal, *J. Am. Chem. Soc.* 2006, **128**, 12299; b) T. Aubert, M. Cirillo, S. Flamee, R. Van Deun, H. Lange, C. Thomsen, Z. Hens, *Chem. Mater.* 2013, **25**, 2388.
7. A. W. H. Lin, J. Y. Ying, *Chem. Mater.* 2010, **22**, 5672.
8. a) J. S. Son, K. Park, S. G. Kwon, J. Yang, M. K. Choi, J. Kim, T. Hyeon, *Small* 2012, **8**, 2394; b) J. S. Son, X.-D. Wen, J. Joo, J. Chae, S.-i. Baek, K. Park, J. Kim, K. An, J. Yu, S. Kwon, S.-H. Choi, Z. Wang, Y.-W. Kim, Y. Kuk, R. Hoffmann, T. Hyeon, *Angew. Chem. Int. Ed.* 2009, **48**, 6861. *Angew. Chem*. 2009**, 121**, 6993.
9. T. Ruberu, A. Purnima, J. Vela, *ACS Nano* 2011, **5**, 5775.
10. S. Ithurria, G. Bousquet, B. Dubertret, *J. Am. Chem. Soc.* 2011, **133**, 3070-3077.
11. A. S. Masadeh, E. S. Božin, C. L. Farrow, G. Paglia, P. Juhas, S. J. L. Billinge, A. Karkamkar, M. G. Kanatzidis, *Phys. Rev. B* 2007, **76**, 11, 115413.
12. Y.-H. Liu, V. L. Wayman, P. C. Gibbons, R. A. Loomis, W. E. Buhro, *Nano Lett.* 2009, **10**, 352.